濟州大學校 尖端技術硏究所 論文集, 第18卷, pp.77-88, 2007. 12
Cheju Nat'l Univ. Res. Inst. Adv. Tech. Jour., Vol.18, pp.77-88, 2007. 12

Sonar Grid Map Based Localization for Autonomous Mobile Robots

Yu-Cheol Lee* · Jong-Hwan Lim**

ABSTRACT

A mobile robot must be able to build a reliable map of surroundings and estimate its position. We have developed a technique for a grid-based localization of a mobile robot with ultrasonic sensors using EKF (Extended Kalman Filter). For this, we used grids themselves as landmarks of the environment. The grid-based localization can minimize the use of computer resources for localization because this approach does not rely on exact geometric representation of a landmark. Experiments were performed in a real environment to verify the methodology developed in this study, and the results indicate that the grid-based localization can be useful for a practical application.

Key Words : Localization, Grid Map, EKF, Sonar, Mobile Robot

Ⅰ. Introduction

An autonomous mobile robot requires a localization technique to move and adapt at an unknown environment [1-3]. The meaning of localization for a mobile robot can be explained as estimating its position to answer the question "Where am I?". To estimate its location, the mobile robot needs a sensor to recognize the surroundings. Many researchers have developed various methods of position estimation by utilizing many kinds of sensors.

Cox originally addressed the localization problem, which is computing an estimation of the mobile robot position when there is a lack of knowledge about the current position of vehicle in the navigation area [4][5]. Cox suggests a localization method using infrared range scanner and an odometer with the mobile robot named Blanche. The positions of the mobile robot were obtained by matching the sensor observation using an initial estimate of vehicle position from odometer according to iterative process.

Hinkel et al., Hoppen et al. and Gonzalez et al. have developed a localization technique using high speed laser rangefinder [6-8]. Hinkel et al. and Hoppen et al. presented a histogram based algorithm that was successfully worked in simple geometry environment such as corridors. Gonzalez et al. proposed an iconic algorithm, where laser ranges were paired with

* Intelligent Robot Research Division, ETRI.
** Faculty of Mechanical, Energy & System Engineering, Cheju National University. Research Institute of Advanced Technology,

a segment based representation of environment. They obtained the mobile robot position from the set of pairings between observations and model features by an error minimization algorithm where a set-based representation of sensor error was considered. However, their algorithms seem to have limitation for the application of sonar sensor because sonar sensor can not acquire the range data as speedy as a laser scanner and the directivity of sonar range data is dissimilar from optical range data such as laser beam information.

Leonard et al. have first developed the model-based localization technique using sonar sensors [9-11]. They suggested the concept of "Regions of constant depth (RCDs)," which was drawn from raw sonar range data. The geometric model is composed of the corner, edge, cylinder and wall and it is constructed by matching between RCDs. The constructed model features are used for robot localization by extended Kalman filter. The results of this method are considered a success when it is applied to the simple environments. However, it can be hardly applied to a dynamic and unknown environment because the feature-based map building method has some limitations.

A problem of feature map is a limitation of geometric representation in the complex environments. For example, the curved shapes of object cannot exactly be represented in the feature map because it is not registered in the feature models. The other limitation is that the feature based-map building method can hardly manage the existing features generated in the past, so that it is difficult to cope with the dynamic environment.

The grid map building method can cover the weak points of the feature map mentioned above. The technique of position estimation based on grid map has been first introduced by Elfes [12][13]. To estimate the robot position, local grid maps were constructed using sonar range data. The robot positions were estimated by finding the best matched positions between local and global maps. However, this approach has a limitation that the robot cannot continuously estimate its position because it is independent of previous movements.

In this study, grid map based localization is presented that is able to continuously estimate the robot's position using sonar data. The grid map based localization algorithm is similar to the feature based localization in a way that it also uses the extended Kalman filter. However, the process of this technique is much simpler than the feature based localization method because the grid map does not require a specific geometric landmark.

The paper also presents the extraction method of robust landmarks from grid map, which should rigidly represent the robot surroundings. The plant model has been developed to predict the robot position using geometric relation of control input. The measurement model has also been developed to match between grid-based landmark and sonar range. The techniques of landmark extraction and mathematical models have been implemented to estimate the robot's position using EKF.

II. Certainty Grid-Based Mapping

A Bayesian probability map is composed of many grids that represent the workspace of the robot. Each grid has an occupancy probability of an object. Fig. 1 shows a sonar footprint, which is assumed to be a fan shape. The grids within the sonar footprint that are to be up-

dated are rearranged according to the distance from the transducer location. These grids are divided into empty regions, e.g., grids *1* through *j−1*, because the sonar beam must pass through them, and into occupied regions, e.g., grids *j* through *j+m*, where the beam stops. The measured range can extend to any cell in the occupied region. The occupancy probability for a grid in the empty region should decrease, while that for a grid in the occupied region should increase. The updated occupancy probability is determined using the Bayes conditional probability theory according to the distance and angle of the grid from the sensor [14].

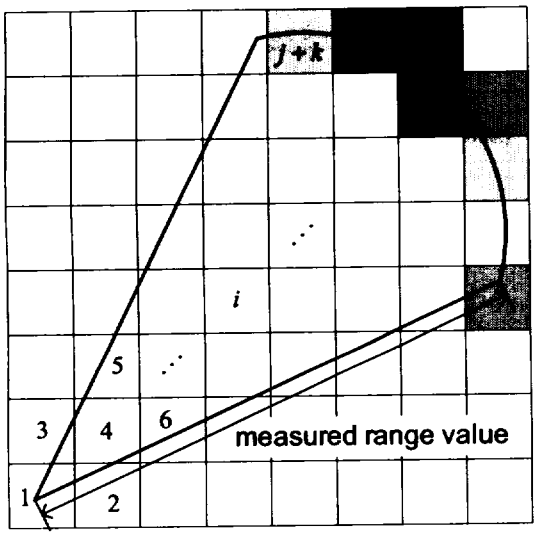

Fig. 1. Footprint of a sonar beam.

The Bayesian model supports a sound theoretical basis for the probability map. In real applications, however, it does not consider specular reflection that frequently returns incorrect range data[15]. In Fig. 1, for example, if specular reflection occurs at the i_{th} grid, the probabilities of the grids behind it (from *i+1* to *j+m*) should not be updated. The Bayesian model, however, still updates those probabilities regardless of the specular reflection. As a result, the occupancy probabilities of the grids corresponding to real objects can become exceedingly small.

To solve this problem, Lim and Cho [15][16] developed a mapping model with the ability to detect specular reflection by evaluating the orientation probability of each grid. In this model, the orientation probability was updated using the specular reflection effect conversely. As shown in Fig. 2, the grid was divided into *n* orientations. The orientation was determined by the relative angle from the sensor bearings, and its probability was updated using the Bayes formula. For example, Fig. 2 shows that only the k_{th} orientation probability increases because the sonar beam must be reflected vertically from the object surface. As the information is accumulated, the probability of the orientation corresponding to a real object surface continuously increases, while those of the rest of the orientations decrease. The possibility that the specular reflection effect or multipath phenomena occurred for each set of sonar range data can be probabilistically considered using the orientation probabilities. Data with a high possibility of the specular reflection have little influence on the occupancy probability updates while data with a low possibility of specular reflection effect have much influence on the occupancy probability updates. Thus, the orientation model can construct a good quality map despite the presence of specular reflection.

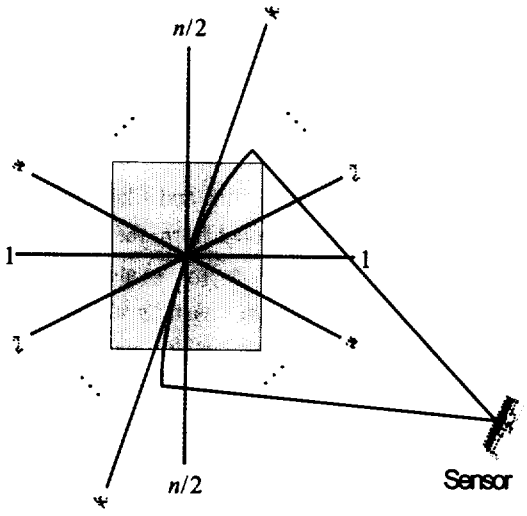

Fig. 2. Virtual orientations in a grid.

III. Certainty Grid-Based Localization

The grid map based localization with occupancy probabilities has been developed to estimate the robot position in this paper. The tool for localization is the EKF (Extended Kalman Filter) that has been extensively used to estimate position such as missile tracking and GPS route navigation of ship. For the application of EKF to a mobile robot, strong landmark should be extracted from robot's surrounding from grid map. This chapter presents the extracting technique of a strong landmark as well as the plant and the measurement models to predict and estimate the robot position with the extracted landmarks.

3.1 Landmark

The selection of a specific landmark is a significant factor that decides the success of the robot localization[17-20]. The landmark plays an important role in the robot localization. As shown in Fig. 3, a sonar beam is expressed as the fan shape because of the angular uncertainty of the sonar sensor, and the point feature are generated where the two sonar footprints from different positions are crossed each other. This point feature can easily detected by a sonar sensor, and the visibility angle, defined as the range of angles from which the feature is detected by the sensor, is larger than that of the a line feature. Therefore, we defined the strong landmark as the point feature. If the occupancy probability of a new point feature is high, then it is selected as a new landmark for localization.

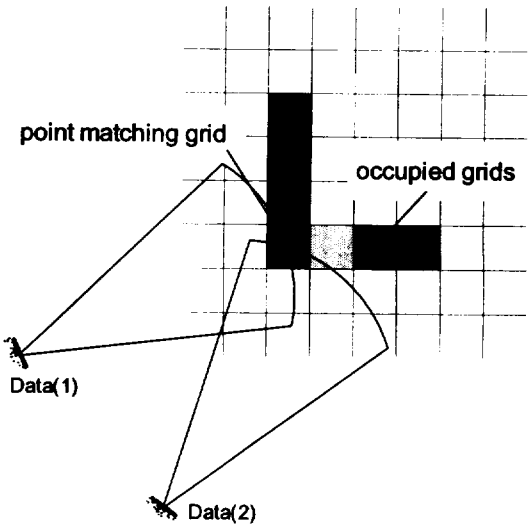

Fig. 3. Representation of a landmark.

3.2 Position Prediction Model

The first step for the estimation of the robot location is to predict the next step of the robot position from the known information of the previous robot position. The k_{th} position of the robot in the two dimensions is defined as $X(k)$ in the Eq. (1). $X(k)$ consists of $x(k)$, $y(k)$ and

orientation $\theta(k)$ on the Cartesian coordinate.

$$X(k)=[x(k), y(k), \theta(k)]^T \quad (1)$$

Therefore, the robot position at $k+1_{th}$ is defined as $X(k+1)$. $U(k)$, the robot's control input, is required to estimate $X(k+1)$. As shown in the Eq. (2), $U(k)$ depends on two factors, translation distance $d(k)$ and rotation angle $\Delta\theta(k)$.

$$U(k)=[d(k),\Delta\theta(k)]^T \quad (2)$$

As shown in Fig. 4, the robot location $X(k+1)$ can be predicted from the geometric analysis of the robot movement using $X(k)$ and $U(k)$. When a robot rotates with an angle of $\Delta\theta(k)$ and then moves with a distance of $d(k)$, the $k+1_{th}$ robot location can be defined as the following.

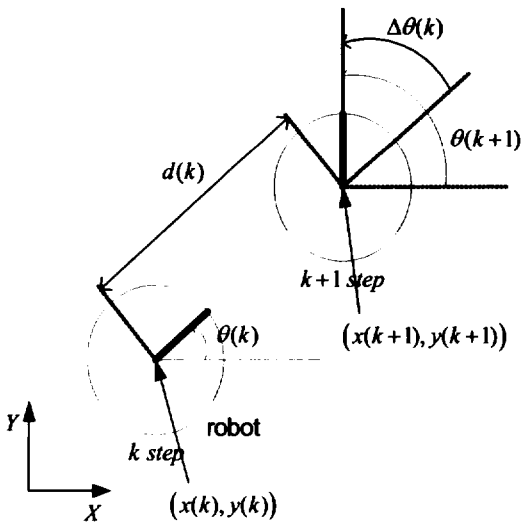

Fig. 4. Position and orientation of a robot at time step k and $k+1$.

$$X(k+1)=f(X(k),U(k))+v(k) \ , \ v(k)\sim N(0,Q(k)) \quad (3)$$

In Eq. (3), $f(X(k),U(k))$ is the plant model of a robot and it can be expressed by the non-linear state transition function as the Eq. (4). Also, $v(k)$ represents the noise source of dead reckoning and it can be expressed by the zero mean Gaussian noise whose mean is 0 and covariance is $Q(k)$ [21].

$$f(X(k),U(k))=\begin{pmatrix} x(k)+d(k)\cos\theta(k) \\ y(k)+d(k)\sin\theta(k) \\ \theta(k)+\Delta\theta(k) \end{pmatrix} \quad (4)$$

The robot position, $X(k+1)$, is unknown due to odometer errors. For this reason, $X(k+1)$ can only be predicted using the estimated kth position, $\hat{x}(k/k)$, and control input, $U(k)$, as shown in Eq. (5).

$$\hat{X}(k+1|k)=f(\hat{X}(k|k),U(k))=\begin{pmatrix} \hat{x}(k)+d(k)\cos\hat{\theta}(k) \\ \hat{y}(k)+d(k)\sin\hat{\theta}(k) \\ \hat{\theta}(k)+\Delta\theta(k) \end{pmatrix} \quad (5)$$

The error between the estimated value, $\hat{x}(k+1/k)$, from the Eq. (5) and the defined value, $X(k+1)$, from the Eq. (3) is expressed as a covariance. At this time, $\hat{x}(k/k)$ is the estimated value while the control input, $U(k)$, is the defined value. Therefore, the error of $\hat{x}(k+1/k)$ can be expressed by the covariance, $C(k+1/k)$, as shown in the Eq. (6) when the robot position $X(k+1)$ from the Eq. (3) is expressed under Taylor Series of the estimated position, $\hat{x}(k/k)$ [22].

$$C(k+1|k)=\nabla f\cdot C(k|k)\cdot\nabla f^T+Q(k) \quad (6)$$

In the Eq. (6), $C(k/k)$ is the covariance of the k_{th} robot position error. ∇f is Jacobian of the state transition function, $f(\hat{x}(k/k),U(k))$, and it is expressed as the Eq. (7).

$$\nabla f = \begin{bmatrix} \frac{\partial f_1}{\partial \hat{x}} & \frac{\partial f_1}{\partial \hat{y}} & \frac{\partial f_1}{\partial \hat{\theta}} \\ \frac{\partial f_2}{\partial \hat{x}} & \frac{\partial f_2}{\partial \hat{y}} & \frac{\partial f_2}{\partial \hat{\theta}} \\ \frac{\partial f_3}{\partial \hat{x}} & \frac{\partial f_3}{\partial \hat{y}} & \frac{\partial f_3}{\partial \hat{\theta}} \end{bmatrix} = \begin{bmatrix} 1 & 0 & -d(k)\sin\left(\hat{\theta}(k)\right) \\ 0 & 1 & d(k)\cos\left(\hat{\theta}(k)\right) \\ 0 & 0 & 1 \end{bmatrix} \quad (7)$$

In the $k+1_{th}$ robot position uncertainty, $C(k+1/k)$, k_{th} covariance, C(k|k), progresses a geometric relation of $\nabla f \cdot C(k/k) \cdot \nabla f^T$, and this means the noise of the control inputs, $d(k)$ and $\Delta\theta(k)$, is added.

3.3 Position Estimation Model

3.3.1 Prediction of Sonar Range Value

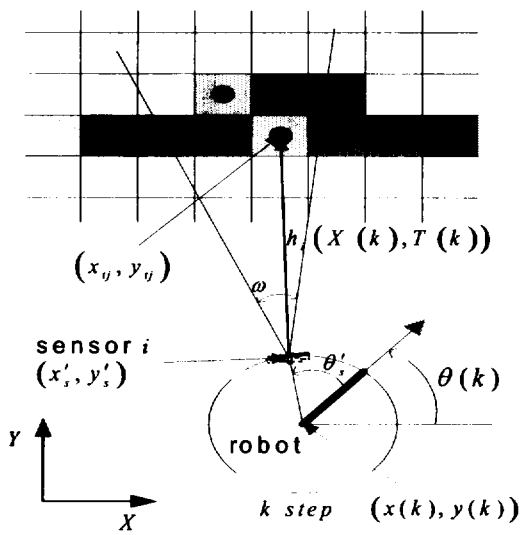

Fig. 5. Global and local sensor locations.

In order to predict sensor ranges at the predicted robot position, $\hat{x}(k+1/k)$, the measurement model should be defined. As shown in Fig. 5, sensor i is defined as the local coordinate frame, $[x'_s, y'_s, \theta'_s]$, that considers robot center as the origin. This can be converted to global coordinate frame, $[x_s(k), y_s(k), \theta_s(k)]$, using Eq. (8).

$$\begin{bmatrix} x_s(k) \\ y_s(k) \\ \theta_s(k) \end{bmatrix} = \begin{bmatrix} x(k) + x'_s\cos\theta(k) - y'_s\sin\theta(k) \\ y(k) + x'_s\sin\theta(k) - y'_s\cos\theta(k) \\ \theta(k) + \theta'_s \end{bmatrix} \quad (8)$$

If the total number of landmarks that sensor i can detect is r, each position of landmark can be defined as Eq. (9).

$$T(k) = \left\{ \left(x_{ij}(k), y_{ij}(k)\right) \mid 0 \le j \le r \right\} \quad (9)$$

Since a sonar sensor detects the nearest landmark, the measurement model can be expressed as the Eq. (10).

$$h_i(X(k),T(k)) = \min\left\{ \sqrt{\left(x_s(k) - x_{ij}(k)\right)^2 + \left(y_s(k) - y_{ij}(k)\right)^2} \mid 1 \le j \le r \right\} \quad (10)$$

In the predicted robot position, $\hat{x}(k+1/k)$, that can be estimated using the measurement model defined in Eq. (10), the sensor i will predict the range reading as,

$$\hat{z}_i(k+1|k) = h_i\left(\hat{X}(k+1|k), T(k+1)\right) \quad (11)$$

3.3.2 Matching of Sonar Information

This is a process to determine the validity of an estimated value, which was obtained by the difference between the predicted observation measurement and the actual sonar measurement. In Fig. 5, the range of sensor i, z_i, can

be defined as Eq. (12).

$$z_i(k)=h_i\left(X(k),T(k)\right)+w_i(k)\quad,\quad w_i(k)\sim N\left(0,R_i(k)\right) \tag{12}$$

The Eq. (12) indicates that the sonar measurement is calculated by the addition of sensor noise to the distance, h_i, when sensor i at the position of $X(k)$ shoots a beam to the landmark $T(k)$. The noise of sensor i, $w_i(k)$, is expressed as the zero mean Gaussian noise whose average is 0 and covariance is defined $R_i(k)$. When the Eq. (12) is applied to the predicted position, $\hat{X}(k+1/k)$ can be expressed using Taylor series such that;

$$z_i(k+1)=h_i\left(\hat{X}(k+1|k),T(k+1)\right)+\frac{\partial h_i}{\partial X}\left[\hat{X}(k+1|k)-X(k+1)\right]+highorderterm+w_i(k+1) \tag{13}$$

If the high order terms except the first order term in the Eq. (13) are neglected, then the equation is linearized as,

$$z_i(k+1)=h_i\left(\hat{X}(k+1|k),T(k+1)\right)+\nabla h_i\cdot\left[\hat{X}(k+1|k)-X(k+1)\right]+w_i(k+1) \tag{14}$$

In Eq. (14), ∇h_i is Jacobian of the measurement model, hi, and it is shown in Eq. (15). d is the closest distance from the predicted sensor position.

$$\nabla h_i=\frac{1}{d}\begin{bmatrix}\hat{x}_i-x_{ij}\\ \hat{y}_i-y_{ij}\\ \left[(x_{ij}-\hat{x}_i)(x_i'\sin\hat{\theta})+y_i'\cos\hat{\theta}+(y_{ij}-\hat{y}_i)(-x_i'\cos\hat{\theta})+y_i'\sin\hat{\theta}\right]\end{bmatrix}^T \tag{15}$$

To determine a validity of the predicted observation measurement, the difference of $zi(k+1)$ in Eq. (14) and $\hat{z}i(k+1/k)$ in Eq. (11) should be calculated.

$$\begin{aligned}\tilde{z}_i(k+1)&=z_i(k+1)-\hat{z}(k+1|k)\\&=\nabla h_i\cdot\left[X(k+1|k)-\hat{X}(k+1|k)\right]+w_i(k+1)\\&=\nabla h_i\cdot\tilde{X}(k+1|k)+w_i(k+1)\end{aligned} \tag{16}$$

The innovation covariance, which is obtained from the Eq. (16), can be expressed as $s_i(k+1)$ in the Eq. (17).

$$s_i(k+1)=\nabla h_i\cdot C(k+1|k)\cdot\nabla h_i^T+R_i(k+1) \tag{17}$$

In Eq. (17), $R_i(k+1)$ indicates the covariance expressing the sensor noise error. Using the innovation, $\tilde{z}_i(k+1)$, in Eq. (16) and the innovation covariance, $s_i(k+1)$, in Eq. (17), it can be evaluated how the predicted observation and the actual sonar measurement are matched in Eq. (18) [10].

$$\tilde{z}_i(k+1)s_i^{-1}(k+1)\tilde{z}_i^T(k+1)\le e^2 \tag{18}$$

In Eq. (18), e is a design parameter to be determined in advance. If matching satisfies the Eq. (18), it is successful. If there are n sonar sensors satisfying the Eq. (18) among the various sonar sensors, the composite innovation can be expressed as following.

$$Z(k+1)=\begin{bmatrix}z_1(k+1)-\hat{z}_1(k+1|k)\\ \vdots\\ z_n(k+1)-\hat{z}_n(k+1|k)\end{bmatrix} \tag{19}$$

Also the Jacobian of composite measurement

model of sonar sensors can be expressed as Eq. (20).

$$\nabla H = \begin{bmatrix} \nabla h_1 \\ \vdots \\ \nabla h_n \end{bmatrix} \tag{20}$$

Using the Eq. (20), the composite innovation covariance can be induced as Eq. (21).

$$S(k+1) = \nabla H \cdot C(k+1|k) \cdot \nabla H^T + R(k+1), \quad R(k+1) = diag\{R_i(k+1) \mid 1 \le i \le n\} \tag{21}$$

In Eq. (21), *R(k+1)* is Gaussian noise of n sonar sensors.

3.3.3 Updating Estimated Position

From the composite innovation calculated above, the robot position and its covariance are updated. The well-known Kalman gain is represented in Eq. (22) [22].

$$W(k+1) = C(k+1|k) \nabla H^T S^{-1}(k+1) \tag{22}$$

Using a composite innovation covariance in Eq. (21) and a Kalman gain, *W(k+1)*, the estimated robot position and its covariance are updated through Eq. (23) and (24).

$$\hat{X}(k+1|k+1) = \hat{X}(k+1|k) + W(k+1) Z(k+1) \tag{23}$$

$$C(k+1|k+1) = C(k+1|k) - W(k+1) S(k+1) W^T(k+1) \tag{24}$$

IV. Experiment and Results

4.1 Experimental Setup and Method

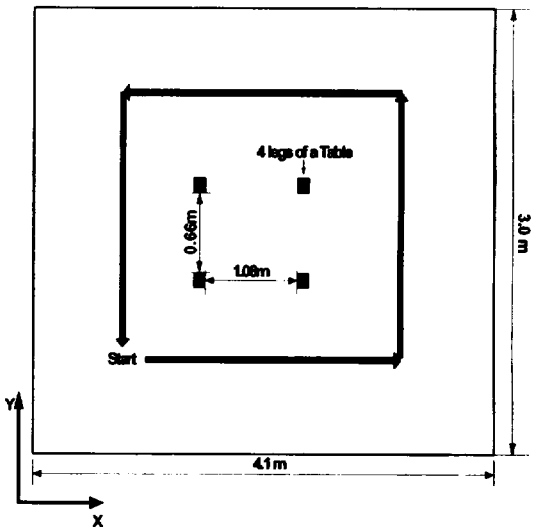

Fig. 6. Experimental environment and the robot's path.

The mobile robot used in the experiment was the Pioneer 3-DX built by the ActiveMedia Robotics Company. This robot consisted of two driving wheels and one non-driving wheel. The traveling distance is measured with two encoders mounted on each driving wheel. A gyroscope was used to measure the rotational angle of the robot. A sonar ring of 16 sensors was mounted on the top of the robot. The experimental environment was composed of a table in the middle of the environment and rectangular walls. That was because a table and a wall could be used as a landmark. The robot was run 6 times along the arrow direction in Fig. 6 with a velocity of 0.05m/s, and the data scanning frequencies were 2 Hz. The size of a grid is 4cm*4cm, and the aperture of sonar sensor was assumed to be 22.5° . Total 42,288 sets of sonar data were acquired from

2643 different robot's positions, and the flow-chart of the localization is shown in Fig. 7. During the first run around the environment, the robot executed map building, landmark selection, and position estimation simultaneously. The rest of navigation was performed based on the landmarks selected during the first run.

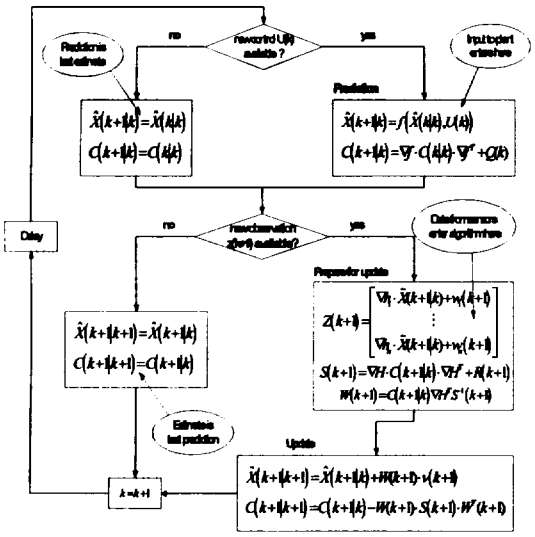

Fig. 7. Flowchart for grid-based localization using EKF algorithm.

4.2 Experimental Results

(a) Initial grid-based map.

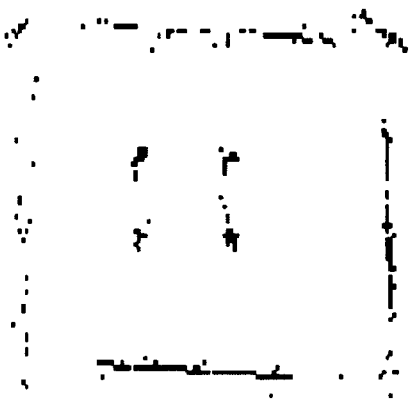

(b) Selected landmarks from the initial map.

Fig. 8. Experimental grid-based map and selected landmarks after 1st run.

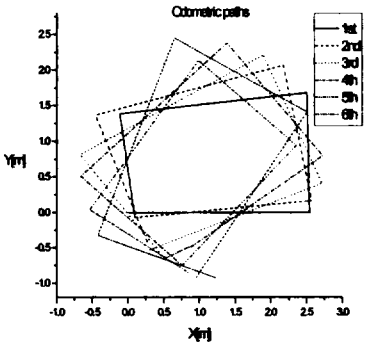

(a) Experimental results of the odometric positions.

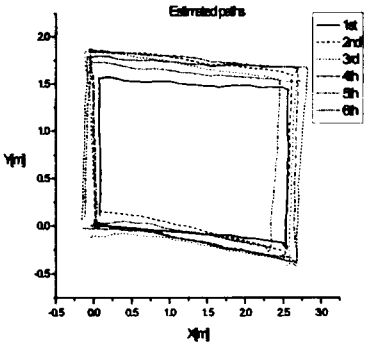

(b) Experimental results of estimated positions.

Fig. 9. Experimental results of localization.

Fig. 8(a) is the constructed grid map when the robot has completed the first run around the experimental surroundings. Looking at the result, it can be said that the probabilities of occupied region and those of empty region are quite different. Fig. 8(b) shows the selected grids as landmarks after the first run. The comparison between the odometric and estimated trajectories are shown in Fig. 9. As shown in the figure, the trajectory from the odometry is distorted due to the accumulated position and heading error of the robot. Fig. 10 shows the resulting maps after 6-th runs, which shows the performance of the localization based on the selected landmarks shown in the Fig. 8. The qualities of the two maps are also quite different, which means the proposed method can be applied effectively for localization of a mobile robot. The position and angle errors during the navigation are shown in Fig. 11. The angle and position errors with only odometry grow over time, while those from estimated positions are bounded.

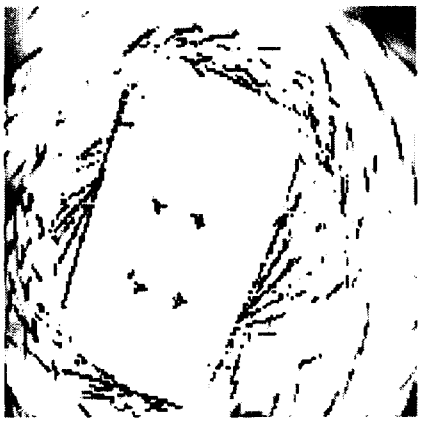

(a) Map building result using odometric posions.

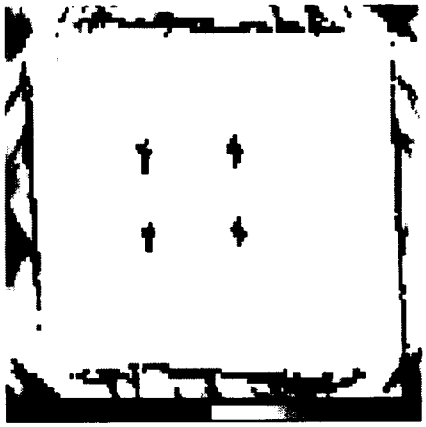

(b) Map building result using estimated positions.

Fig. 10. Map building results after 6th run.

V. Conclusion

In this study, grid map based localization was presented that is able to continuously estimate the robot's position using sonar data. We have developed a technique for a grid-based localization of a mobile robot with ultrasonic sensors using EKF (Extended Kalman Filter). For this, we used grids themselves as landmarks of the environment. The grid-based localization can minimize the use of computer resources for localization because this approach does not rely on exact geometric representation of a landmark. The grid map based localization algorithm is similar to the feature based localization in a way that it also uses the extended Kalman filter. However, the process of this technique is much simpler than the feature based localization method because the grid map does not require a specific geometric landmark. The paper also presented the extraction method of robust landmarks from a grid map. Experiments were performed in a real envi-

ronment to verify the methodology developed in this study, and the results have shown that the grid-based localization can be useful for a practical application.

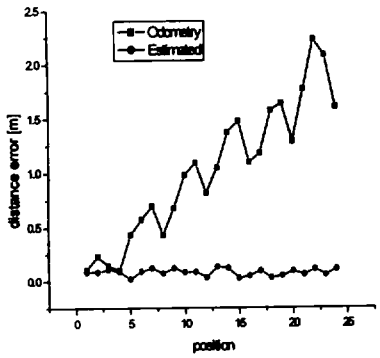

(a) Distance error

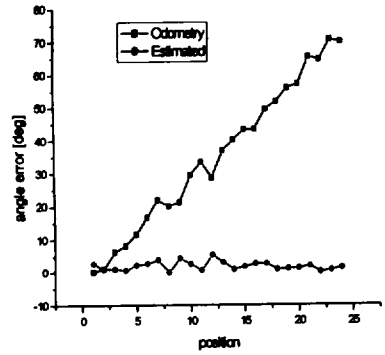

(b) Angle error.

Fig. 11 Characteristics of position error.

References

[1] R. Smith, M. Self, and P. Cheeseman, 1987, "A stochastic map for uncertain spatial relationships," 4th International Symposium on Robotic Research, MIT Press.

[2] M. Dissanayake, P. Newman, S. Clark, H. F. Durrant-Whyte, and M. Csorba, 2001, "A solution to the simultaneous localization and map building problem," IEEE Trans. on Robotics and Automation, Vol.17, No.3, pp. 229-241.

[3] J. D. Tards, J. Neira, P. M. Newman, and J. J. Leonard, 2002, "Robust mapping and localization in indoor environments using sonar data", International Journal of Robotics Research, Vol.21, No.4, pp.311-330.

[4] I. J. Cox, 1988, "Blanche: An autonomous robot vehicle for structured environments", Proc. IEEE Int. Conf. Robotics and Automation, pp.978-982, Philadelphia, PA, USA.

[5] I. J. Cox, 1991, "Blanche an experimental in guidance and navigation of an autonomous robot vehicle." IEEE Trans. Robotics and Automation, Vol.7, No.2, pp.193-204.

[6] R. Hinkel, T. Knieriemen and E. Puttkamer, 1988, "Mobot-III an Autonomous Mobile Robot for Indoor Applications", Proceedings of the International Symposium and Exhibition on Robots, pp.489-504, Sydney, Australia.

[7] P. Hoppen, T. Knieriemen and E. Puttkamer, 1990, "Laser-Radar Based Mapping and Navigation for an Autonomous Mobile Robot", Proc. IEEE Int. Conf. Robotics and Automation, pp.948-953, Cincinnati.

[8] J. Gonzalez, A. Stentz, and A. Ollero, 1992, "An iconic position estimator for a 2D laser rangefinder", Proc. IEEE Int. Conf. Robotics and Automation, pp.2646-2651, Nice, France.

[9] J. J. Leonard and H. F. Durrant-Whyte, 1991, "Mobile Robot Localization by Tracking Geometric Beacons", IEEE Trans. on Robotics and Automation, Vol.7, No.3, pp.513-523.

[10] J. J. Leonard, 1990, "Direct Sonar Sensing for Mobile Robot Navigation", Kluwer Academin.

[11] J. H. Lim and J. J. Leonard, 2000, "Mobile Robot Relocation from Echolocation Constraints", IEEE Trans. on Pattern Analysis and Machine Intelligence, Vol.22, No.9, pp. 10351041.

[12] H. Moravec and A. Elfes, 1985, "High resolution maps from wide angle sonar", Proc. IEEE Int. Conf. Robotics and Automation, St.Louis, pp.116-121.

[13] A. Elfes, 1987, "Sonar-based Realworld Mapping and Navigation", IEEE Transactions on Robotics and Automation, Vol.3 No.4, pp.249-265.

[14] D. W. Cho and H. P. Moravec, 1989, "A Bayesian Method for Certainty Grids", AAAI Spring Symposium on Robot Navigation, Stanford, CA, pp.57-60.

[15] J. H. Lim and D. W. Cho, 1996, "Multi-path Bayesian Map Construction Model from Sonar Data", ROBOTICA, Vol.14, pp. 527-540.

[16] J. H. Lim, 1994, "Map Construction, Exploration, and Position Estimation for an Autonomous Mobile Robot using Sonar Sensors", Ph.D thesis, Pohang Institute of Science and Technology, Korea.

[17] O. Wijk and H. I. Christensen, 2000, "Triangulation-Based Fusion of Sonar Data with Application in Robot Tracking", IEEE Trans. on Robotics and Automation, Vol.16, No.6, pp.740-752.

[18] K. Nagatani and H. Choset, 1999, "Toward robust sensor based exploration by constructing reduced generalized Voronoi graph", Proc. of IEEE/RSJ Int. Conf. on Intelligent Robots and Systems, pp.1687 -1692.

[19] H. Choset, K. Nagatani, and N. A. Lazar, 2003, "The Arc-Transversal Median Algorithm: A Geometric Approach to Increasing Ultrasonic Sensor Azimuth Accuracy," IEEE Trans. on Robotics and Automation, Vol.19, No.3, pp.513-522.

[20] L. Kleeman and R. Kuc, 1994, "An optimal sonar array for target localization and classification," IEEE International Conference on Robotics and Automation, pp.3130-3135.

[21] A. C. Gelb, 1973, "Applied Optimal Estimation", The MIT Press.

[22] Y. Bar-Shalom, T. E. Fortmann, 1988, "Tracking and Data Association", Academic Press.